THE JOURNAL OF PHYSICAL CHEMISTRY A

Article

pubs.acs.org/JPCA

Site-Specific Electron-Relaxation Caused by Si:2p Core-Level Photoionization: Comparison between $F_3SiCH_2CH_2Si(CH_3)_3$ and $Cl_3SiCH_2CH_2Si(CH_3)_3$ Vapors by Means of Photoelectron Auger Electron Coincidence Spectroscopy

Shin-ichi Nagaoka,*[,†] Takuhiro Kakiuchi,[†] Joji Ohshita,[‡] Osamu Takahashi,[§] and Yasumasa Hikosaka[∥]

[†]Department of Chemistry, Faculty of Science and Graduate School of Science and Engineering, Ehime University, Matsuyama 790-8577, Japan

[‡]Department of Applied Chemistry, Graduate School of Engineering and [§]Institute for Sustainable Sciences and Development, Hiroshima University, Higashi-Hiroshima 739-8511, Japan

[∥]Graduate School of Medicine and Pharmaceutical Sciences, University of Toyama, Toyama 930-0194, Japan

Supporting Information

ABSTRACT: Site-specific electron relaxations caused by Si:2p core-level photoionizations in $F_3SiCH_2CH_2Si(CH_3)_3$ and $Cl_3SiCH_2CH_2Si(CH_3)_3$ vapors have been studied by means of the photoelectron Auger electron coincidence spectroscopy. $F_3SiCH_2CH_2Si(CH_3)_3$ shows almost 100% site-specificity in fragmentation caused by the Si:2p ionization. However, substitution of Cl for F of $F_3SiCH_2CH_2Si(CH_3)_3$ considerably reduces the site-specificity at the Si atom bonded to three halogen atoms, with the site-specificity at the Si site bonded to three methyl groups remaining largely unchanged. The site-specificity reduction in $Cl_3SiCH_2CH_2Si(CH_3)_3$ is considered to take place during the transient period between Si:L_{23}VV Auger electron emission and the subsequent fragmentation. The reason for the reduction can be explained in terms of some differences between these two molecules in the L_{23}VV Auger decay at the Si site bonded to the three halogen atoms.

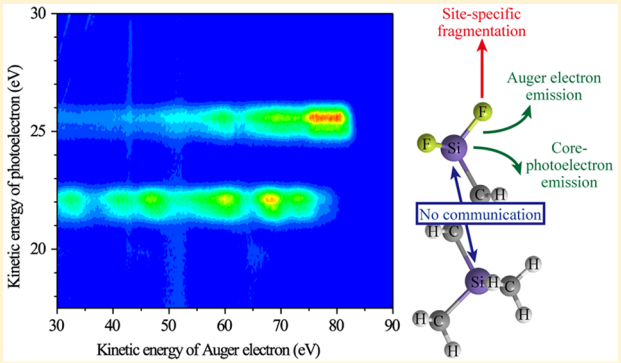

1. INTRODUCTION

Is there any communication between two atoms at either end of a molecule? The answer is often "No!" in fragmentation caused by core-level photoionization.[1−3] Because a core electron is localized very close to the nucleus of one particular atom, the core-level photoionization at the left-hand-side atom inside the molecule frequently causes localized bond dissociation around the atom. Then, chemical bonding remains unchanged around the right-hand-side atom with different chemical environment. Like this, in the core-level photoionization and the subsequent fragmentation, the right-hand-side atom inside the molecule, so to speak, does not know what is being done at the left-hand-side atom, in contrast to photoexcitation of a valence electron delocalized over the entire molecule. Such fragmentation caused by the core-level photoionization is called site-specific fragmentation and is promising for controlling chemical reactions at an atomic level.[2,3] The site-specific fragmentation is expected to play a role of "molecular knife" that is an appropriate tool for "cutting" a molecule, a molecular assembly, or a nanoscale device.[3]

Bridged (trihalosilyl)(trimethylsilyl) molecules ($X_3SiC_nH_mSi(CH_3)_3$, X = F or Cl, n = 0−2, and m = 0−4) are useful for studies of the site-specific fragmentation caused by the core-level photoionization, because the chemical environment of the left-hand-side Si atom bonded to three halogen atoms (here denoted Si[X]) is very different from that of the right-hand-side Si atom bonded to three methyl groups (Si[Me]).[3] In fact, whereas the halogen atom is an electron acceptor with a large electronegativity, the methyl group is an electron donor with a small electronegativity.[4] Furthermore, the site-specific fragmentation of Si-containing molecules such as $X_3SiC_nH_mSi(CH_3)_3$ draws much attention, because Si materials are widely used for fabrication of electronic devices and this fabrication has become very precise in recent years.[5]

We previously studied the site-specific fragmentation of $X_3SiC_nH_mSi(CH_3)_3$ vapors by means of the energy-selected-photoelectron photoion−photoion triple-coincidence spectroscopy (PEPIPICO) and photoelectron−photoion coincidence spectroscopy (PEPICO).[3,6,7] Upon Si:2p core-level photoionization, $X_3SiC_nH_mSi(CH_3)_3$ showed two core photoelectron

Received: September 17, 2016
Revised: November 13, 2016
Published: November 28, 2016

DOI: 10.1021/acs.jpca.6b09399
J. Phys. Chem. A 2016, 120, 9907−9915

peaks reflecting the binding-energy difference between the Si[X] and Si[Me] sites. In the subsequent normal Auger transition, a valence electron fell into the Si:2p core orbital and created a valence hole that spatially overlapped the initially core-ionized Si site ($X_3SiC_nH_mSi(CH_3)_3^+$). The electron falling into the Si:2p core orbital gave its energy to another nearby valence electron, which was emitted as a normal Auger electron (two-step model), creating another valence hole near by ($X_3SiC_nH_mSi(CH_3)_3^{2+}$). Because these valence holes weakened chemical bonds around the initially core-ionized Si site, the site-specific fragmentation ($X_3SiC_nH_mSi(CH_3)_3^{2+} \rightarrow F_1^+ + F_2^+$, where F_1^+ and F_2^+ denote fragment ions) often occurred around the Si site. In fact, the experimental results clearly showed almost 100% site specificity in fragmentation caused by the Si:2p photoionization of $F_3SiC_nH_mSi(CH_3)_3$ with a long intersite bridge ($-C_nH_m-$), which was found to prevent intramolecular electron migration between the two Si sites. Such high site specificity in the fragmentation was observed at both of the Si[F] and Si[Me] sites.

However, substitution of Cl for F in $X_3SiC_nH_mSi(CH_3)_3$ reduced the maximum site specificity at the Si[X] site by no less than 50%, with the maximum site specificity at the Si[Me] site remaining largely unchanged (Figures 7 and 8 of ref 3). Of course the electronegativity of Cl is less than that of F and nearer to that of CH_3,[4] but 2p binding energies of the Si[Cl] and Si[Me] sites were clearly separated from each other even after the substitution (Figures S3 and S6 of ref 3). Nevertheless, why did the site specificity in the fragmentation caused by the Si[X]:2p ionization drop much more than that by the Si[Me]:2p ionization? When did the site-specificity reduction take place during relaxation after the Si[Cl]:2p ionization in $Cl_3SiC_nH_mSi(CH_3)_3$? The answers to these questions have not yet been worked out, although such works are essential not only for full understanding of the site-specific fragmentation but also for controlling chemical reactions at an atomic level and realizing the molecular knife.

Accordingly, in the work presented here, we have attempted to elucidate when and why the site-specificity reduction by the F → Cl substitution occurs at the Si[X] site of $X_3SiC_nH_mSi(CH_3)_3$. Answer candidates for the when-done-it are transient periods among (1) core photoelectron emission, (2) Auger electron emission, and (3) fragmentation. As mentioned above, we already studied process 3 being site-selectively caused by process 1, which is to say correlation between processes 1 and 3, in $X_3SiC_nH_mSi(CH_3)_3$ vapors by means of PEPIPICO and PEPICO.[3,6,7] We also investigated correlation between processes 2 and 3 by the Auger electron photoion−photoion triple-coincidence spectroscopy (AEPIPICO) and Auger electron photoion coincidence spectroscopy (AEPICO). Here, to examine correlation between processes 1 and 2, we have compared photoelectron Auger electron coincidence spectra of 1-(trifluorosilyl)-2-(trimethylsilyl)ethane ($F_3SiCH_2CH_2Si(CH_3)_3$, FSMSE) and 1-(trichlorosilyl)-2-(trimethylsilyl)ethane ($Cl_3SiCH_2CH_2Si(CH_3)_3$, CSMSE) vapors. The comparison has elucidated when and why the site specificity is reduced in the fragmentation caused by the Si[Cl]:2p ionization of $Cl_3SiC_nH_mSi(CH_3)_3$. This is the first time that the site-resolved correlation between processes 1 and 2 has been observed in $X_3SiC_nH_mSi(CH_3)_3$ vapor.

2. EXPERIMENTAL SECTION

Preparation methods of FSMSE and CSMSE were reported previously.[8] Each of FSMSE and CSMSE was degassed by means of the repeated pump-thaw method prior to measurements.

On beamline BL4B at UVSOR synchrotron-radiation facility,[9] our experiments were performed during single bunch operation, which provided light pulses with a repetition period of 178 ns and a width of 110 ps. The synchrotron radiation being emitted from a bending magnet of the storage ring was monochromatized by a grazing-incidence monochromator equipped with a varied-line-spacing plane-grating. We used no optical filters for light order sorting.

All the photoelectron Auger electron coincidence measurements of FSMSE and CSMSE vapors were carried out with Y.H.'s home-built magnetic-bottle electron spectrometer whose design and capability had been described elsewhere.[10] Briefly, photoelectrons and Auger electrons created by photoionization of each sample gas were captured over a 4π solid angle by magnetic field lines formed inside the spectrometer and were guided toward a microchannel-plate detector terminating a 1.5-m flight path. Electron signals from the detector were fed, after amplification and discrimination, into a time-to-digital converter (Roentdek TDC8) operated in the multistart common-stop mode. The converter was started by the first-arrived electron-signal, recording the arrival times of the following electrons, and was stopped, after a 10 μs delay, by a master clock signal for the storage ring operation. The time intervals between the stop time and the arrival times of all the electrons during the ∼10 μs time window were evaluated and converted to seeming electron time-of-flights with resetting the start time to the relevant light-pulse incident-time before the first arrival of the electron signal. Because the light pulse was incident on the sample vapor with a repetition period of 178 ns, the seeming electron-time-of-flight from this start time is expressed by the sum of $k \times 178$ ns ($k \geq 0$) and the correct time-of-flight[11] that the electron needed to travel the 1.5 m flight path. If $k = 0$, the electron creation coincided with the start time. If $k > 0$, the electron was created $k \times 178$ ns after the start time, and the seeming time-of-flight then obtained may induce a false structure in the spectrum.

The conversion factor from the correct time-of-flight to the electron kinetic energy was calibrated by using Ar:2p photoelectron spectra (PES)[11] measured at various photon energies. The kinetic-energy resolving power ($E/\Delta E$) being estimated from the photoelectron peaks gave a nearly constant value 35 over the whole kinetic-energy region in the measurement, where E and ΔE denote the electron kinetic energy and bandwidth, respectively. From coincidence yields observed between the Ar:2p photoelectrons and the corresponding normal LMM Auger electrons,[12] the electron detection efficiency was estimated to be ∼50%.

An advantage of the photoelectron Auger electron coincidence spectroscopy is that the coincidence data allow us to identify the source of features in the Auger electron spectrum (AES).[13,14] The coincidence experiment provides an opportunity to find the relationship between the PES and AES peaks. Accordingly, even if the total AES is not clearly resolved site by site in each of FSMSE and CSMSE, it is possible to identify Si[X]- and Si[Me]-site-specific Auger decay processes that may contribute to the Auger peak intensity or modify the peak shape. This coincidence spectroscopy is one of the few means of separating out the relative importance of the two site-specific processes in particular Auger peaks, and is suitable for our purpose. At one time, a disadvantage of this spectroscopy was a long data-collection time, and Thurgate hoped that the

DOI: 10.1021/acs.jpca.6b09399
J. Phys. Chem. A 2016, 120, 9907−9915

time to produce a sensible spectrum would decrease to several hours.[13] In our measurements, this problem has been solved by adopting the magnetic-bottle electron-spectrometer with a high electron-collection efficiency.[10,15]

3. COMPUTATIONAL METHOD AND PROCEDURE

To elucidate the site-specific fragmentation process in detail, we deduced characters of doubly charged states formed after the above-mentioned process (2) (Auger final states) in FSMSE, CSMSE, SiF_4, and $SiCl_4$ by using the ab initio molecular-orbital (MO) method. The geometries of FSMSE, CSMSE, SiF_4, and $SiCl_4$ were optimized out by using GAUSSIAN 09 program[16] at the MP2/cc-pVDZ level of theory to obtain their equilibrium structures.

The basic computational method and procedure used in the ab initio MO calculation of $L_{23}VV$ AES at a Si atom were described in detail in previous papers.[3,17] A set of MOs for the Auger final states was selected out of MOs for the ground state, which were a better choice than those for the Si:2p core−hole state. The energies of the Auger final states were calculated by using the configuration interaction (CI) method within the valence-two-hole space. The intensities of the Auger transition rates were obtained from the electron population analysis.[17] The probabilities of the Auger transitions to all the singlet and triplet states were taken into account in this study.

A computational AES was constructed by Gaussian convolution of the line spectrum thus obtained. The Gaussian functions used there had a full-width-at-half-maximum (fwhm) being given as $(E/80)+\Delta$, where E and Δ denote the Auger electron kinetic energy and fixed bandwidth, respectively. The Δ's were set to 1.5 and 2.0 eV for FSMSE and CSMSE, respectively. The resultant computational AES was energy-shifted so as to facilitate comparison with the corresponding experimental AES.

4. RESULTS AND DISCUSSION

4.1. Correlation between Photoelectron and $L_{23}VV$ Auger Electron Emissions. Figure 1 shows two-dimensional contour representation of correlation between photoelectron and $L_{23}VV$ Auger electron emissions caused by Si:2p core-level photoionization in FSMSE and CSMSE vapors. The vertical axis (y axis) indicates the kinetic energy of the slow electron of the two emitted electrons, and the horizontal axis (x axis) indicates that of the fast electron. Under our experimental conditions, the photoelectron and $L_{23}VV$ Auger electron are emitted as the slow and fast electrons, respectively. When a photoelectron emission with a kinetic energy of y eV induces an Auger electron emission with that of x eV, the photoelectron emission is correlated with (in coincidence with) the Auger electron emission, and one count is added to the contour value $f(x,y)$ at the coordinate (x, y) in Figure 1. The two bars shown in each of Figure 1a,b correspond to two Si:2p-photoelectron peaks reflecting the binding-energy difference between the Si[X] and Si[Me] sites (X = F or Cl).

By summing up the contour values over x ($g_1(y) = \sum_x f(x,y)$), we can extract a Si:2p photoelectron spectrum (PES) from each of Figure 1a,b (y vs $g_1(y)$ plot). Parts a and b of Figure 2 respectively show the Si:2p PES of FSMSE and CSMSE vapors, and the Si[X] and Si[Me] sites of each molecule exhibit energy-resolved Si:2p-photoelectron peak groups at lower and higher kinetic-energy sides. Each of those peak groups is seen to be further split into two components, which come from spin−orbit coupling. The binding energies of Si[X]: and Si[Me]:2p electrons in FSMSE and CSMSE vapors have already been reported (ref 18 and Table S1 of ref 3).

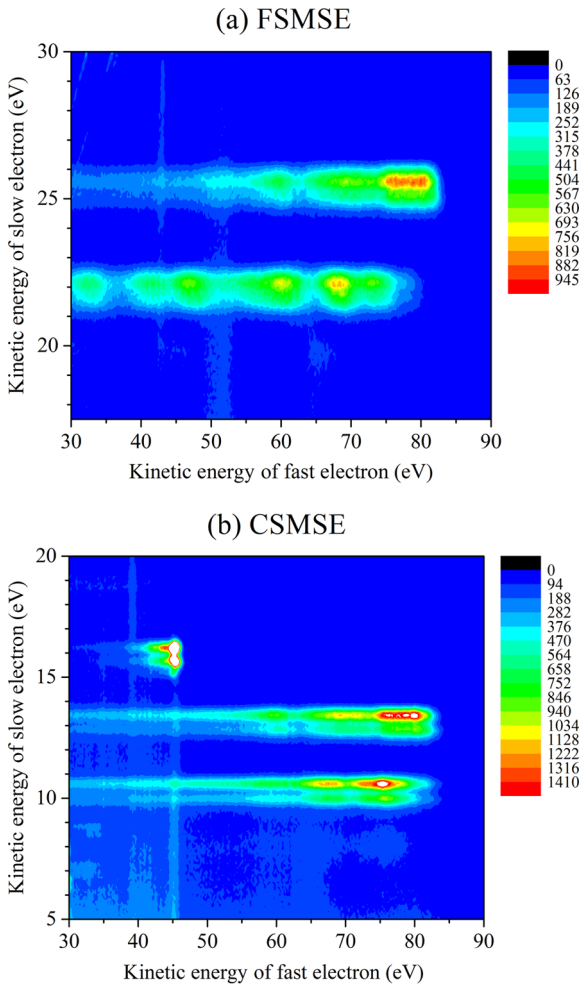

Figure 1. Two-dimensional contour representation of correlation between photoelectron and $L_{23}VV$ Auger electron emissions in Si:2p core-level photoionization. Here, the k value defined in section 2 is zero except for the false structure mentioned below. (a) FSMSE vapor. This spectrum has been measured at a photon energy ($h\nu$) of 131.9 eV. (b) CSMSE vapor and $h\nu$ = 119.5 eV. The island seen around a coordinate value of x = 45 eV and y = 16 eV is a false structure, where the x- and y-axes are taken to be horizontal and vertical, respectively. The k value for the false structure is one, and there Cl:2p core-level photoionization due to the second-order light ($h\nu$ = 239.0 eV) in CSMSE has caused the photoelectron $L_{23}VV$ Auger electron coincidence, whose correct two-dimensional contour representation is given in the Supporting Information (Figure S1).

By summing up the contour values over y ($g_2(x) = \sum_y f(x,y)$), a normal Si:$L_{23}VV$ AES can be extracted from each of Figure 1a and Figure 1b (x vs $g_2(x)$ plot, Figures 3a and 4a). In contrast to the Si:2p PES shown in Figure 2, the Si:$L_{23}VV$ AES is not clearly resolved site by site. The normal Auger transitions produce various doubly charged states (Auger final states). As the Auger electron kinetic energy decreases in Figures 3 and 4, the Auger decay leads to a higher-lying Auger final state with one or two inner valence holes as shown in Figure 5.[19] To examine site-specific electron relaxation in detail, we have to observe Si[XR]:$L_{23}VV$ Auger emission caused by Si[XR]:2p photoelectron emission (XR = F, Cl, or Me).

DOI: 10.1021/acs.jpca.6b09399
J. Phys. Chem. A 2016, 120, 9907−9915

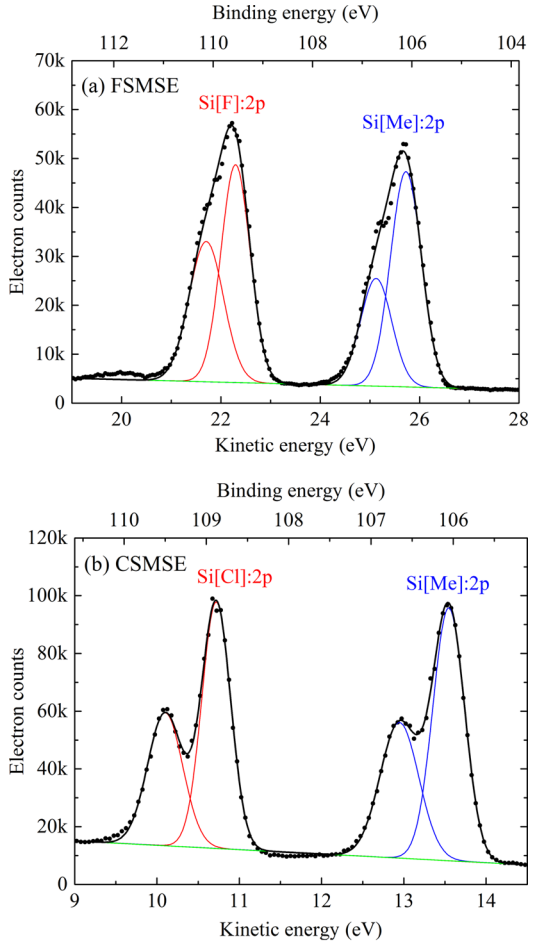

Figure 2. Si:2p PES (dots) obtained by summing up the contour values along the horizontal axis in Figure 1. The red, blue, and green thin profiles indicate results of Gaussian fitting, and the black thick curve is the summation of the thin profiles. (a) FSMSE vapor. Calibration of the binding-energy scale has been performed using a high-resolution Si:2p PES reported previously.[18] The intensity ratios between the $2p_{3/2}$ and $2p_{1/2}$ photoelectrons seen in this figure are 2.0:1.0 and 2.0:1.5 at the Si[Me] and Si[F] sites, respectively. (b) CSMSE vapor. Calibration of the binding-energy scale has been performed using a low-resolution Si:2p PES reported previously (see Table S1 of ref 3). The binding energies of the Si[Me]:$2p_{3/2}$, Si[Me]:$2p_{1/2}$, Si[Cl]:$2p_{3/2}$, and Si[Cl]:$2p_{1/2}$ electrons have been determined to be 106.1, 106.7, 108.9, and 109.5 eV, respectively. The intensity ratios between the $2p_{3/2}$ and $2p_{1/2}$ photoelectrons seen in this figure are 2.0:1.3 at both of the Si[Me] and Si[F] sites. The spectral resolution of this PES is higher than that in Figure 2a.

In the case that the summation $\sum_y f(x,y)$ is made within one of the two bars seen in each of the two-dimensional contour plots in Figure 1, a Si[XR]:2p photoelectron Si[XR]:L_{23}VV Auger electron coincidence spectrum can be extracted. The coincidence spectrum represents the Si[XR]:L_{23}VV Auger emission caused by the Si[XR]:2p photoelectron emission. Figures 3b,c and 4b,c show those coincidence spectra of FSMSE and CSMSE vapors, together with the computational spectra. The summation of the computational Si[X]:L_{23}VV and Si[Me]:L_{23}VV Auger electron spectra (AES) in each molecule is given in Figures 3a and 4a. For comparison, Figures 3 and 4 also represent Si:L_{23}VV AES of $Si(CH_3)_4$, SiF_4, and $SiCl_4$ vapors obtained previously.[20−22] The computational spectra of FSMSE and CSMSE given in Figures 3 and 4 are fairly

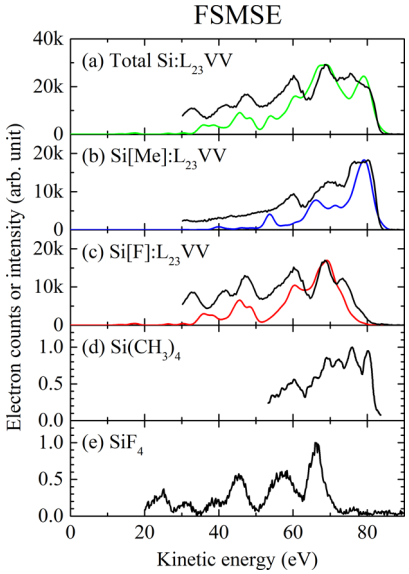

Figure 3. Si:L_{23}VV AES of FSMSE, $Si(CH_3)_4$, and SiF_4 vapors. The experimental AES (black curves) of FSMSE have been extracted from Figure 1a. Each computational spectrum is drawn in color except black. (a) Si:L_{23}VV AES obtained by summing up the contour values along the vertical axis (y axis) in Figure 1a. Summation of Si[F]:L_{23}VV and Si[Me]:L_{23}VV AES of FSMSE. (b) Si[Me]:L_{23}VV Auger emission caused by Si[Me]:2p photoelectron emission in FSMSE. The experimental spectrum has been obtained by summing up the contour values over y = 24.2−26.5 eV in Figure 1a. (c) Si[F]:L_{23}VV Auger emission caused by Si[F]:2p photoelectron emission in FSMSE. The experimental spectrum has been obtained by summing up the contour values over y = 20.6−23.1 eV in Figure 1a. (d) $Si(CH_3)_4$.[21] (e) SiF_4.[20]

consistent with the experimental spectra. The spectra of FSMSE vapor (Figure 3a−c) are similar to those obtained for condensed $F_3SiCD_2CH_2Si(CH_3)_3$.[23]

4.2. Peak Assignments of Site-Specific AES. *4.2.1. Si[Me]:L_{23}VV AES of FSMSE and CSMSE.* Because the Si[Me]:L_{23}VV AES of FSMSE and CSMSE (Figures 3b and 4b) are close to each other and similar to that of $Si(CH_3)_4$ vapor except the spectral resolution (Figures 3d and 4d),[21,24] we can assign the Si[Me]:L_{23}VV Auger peaks seen in both FSMSE and CSMSE according to the data of $Si(CH_3)_4$.[24] The Si[Me]:L_{23}VV Auger peaks in 67−83 eV (Figures 3b and 4b) are assigned to Auger final states with two valence holes delocalized over the four Si[Me]−C bonds. Note that the Si[Me]−C bonding orbitals are polarized, if anything, toward the Si[Me] atom, because each of the alkyl groups bonded to Si[Me] is an electron donor with a small electronegativity.[4] Accordingly, the holes created by the Si[Me]:L_{23}VV Auger decay appear with their principal density around the Si[Me] atom.

4.2.2. Si[F]:L_{23}VV AES of FSMSE. In Figure 3c, FSMSE shows a Si[F]:L_{23}VV Auger peak at 73.4 eV, which comes from hole creation in higher-lying Si[F]−CH_2(bridge) bonding orbitals[25] and appears as a shoulder in the computational Si[F]:L_{23}VV AES. Except for the peak at 73.4 eV, the Si[F]:L_{23}VV AES of FSMSE (Figure 3c) is similar to the Si:L_{23}VV AES of SiF_4 (Figure 3e).[20,26] Furthermore, the Si atom of SiF_4 can be regarded as a model of the Si[F] site in FSMSE.[27] Thus, we have assigned the five Si[F]:L_{23}VV Auger peaks of FSMSE seen in 30−71 eV (Figure 3c) according to an assignment result for SiF_4 by Aksela et al.[26] and a somewhat-revised assignment result based on ab initio MO calculations of SiF_4 by Tarantelli

DOI: 10.1021/acs.jpca.6b09399
J. Phys. Chem. A 2016, 120, 9907−9915

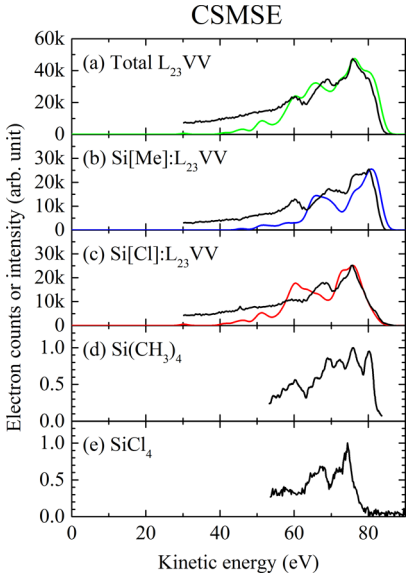

Figure 4. Si:L_{23}VV AES of CSMSE, $Si(CH_3)_4$, and $SiCl_4$ vapors. The experimental AES (black curves) of CSMSE have been extracted from Figure 1b. Each computational spectrum is drawn in color except black. (a) Si:L_{23}VV AES obtained by summing up the contour values along the vertical axis (y axis) in Figure 1b. Summation of Si[Cl]:L_{23}VV and Si[Me]:L_{23}VV AES of CSMSE. (b) Si[Me]:L_{23}VV Auger emission caused by Si[Me]:2p photoelectron emission in CSMSE. The experimental spectrum has been obtained by summing up the contour values over y = 12.3−14.0 eV in Figure 1b. (c) Si[Cl]:L_{23}VV Auger emission caused by Si[Cl]:2p photoelectron emission in CSMSE. The experimental spectrum has been obtained by summing up the contour values over y = 9.4−11.2 eV in Figure 1b. (d) $Si(CH_3)_4$.[21] (e) $SiCl_4$.[22]

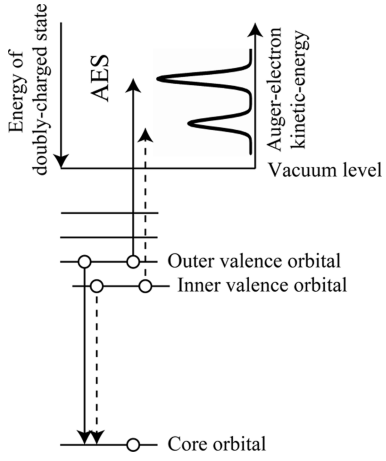

Figure 5. Energy level diagram of some MOs and doubly charged states (Auger final states) related to normal AES. The solid arrows show an outer valence orbital → core−hole transition and the subsequent Auger electron emission from the outer valence orbital. The broken arrows correspond to a case that an inner valence orbital participates in the Auger decay.

et al.[28,29] A similar calculation of FSMSE is very difficult because FSMSE is much larger in molecular size than SiF_4.[30,31]

Note that Si−F bonding orbitals in SiF_4 are polarized toward the F atom in contrast to the Si[Me]−C orbitals mentioned above, because F is an electron acceptor with a large electronegativity.[4] Accordingly, valence holes created by the Si:L_{23}VV Auger decay in SiF_4 appear with their principal density around the F atoms, although the Auger decay is localized at the Si atom as explained for $X_3SiC_nH_mSi(CH_3)_3$ in the Introduction. By performing ab initio Green's-function calculations, Tarantelli et al. showed that pronounced hole localization on one or two of four Si−F bonds takes place in all the Si:L_{23}VV Auger final states of SiF_4.[28,29] The hole-localization phenomena cannot be described within a framework in the absence of two-hole configuration mixing.[30] From the above-mentioned similarity between Figure 3c and Figure 3e, it is considered that similar hole-localization phenomena take place also in the Si[F]:L_{23}VV Auger decay of FSMSE.

Our assignment for FSMSE is schematically summarized in Figure 6a. The Si[F]:L_{23}VV Auger peak-groups of FSMSE seen in 55−71 and 30−50 eV (Figure 3c) are respectively assigned to Auger final states with two outer valence holes located in one or two Si−F bonds and to those with one outer hole and one inner hole located in the Si−F bonds. Each of those two peak groups (55−71 and 30−50 eV) is further split into two or three components. The peaks at 68.6 and 47.4 eV are assigned to Auger final states with one hole located in a Si−F bond and one hole in another Si−F bond, and the peaks at 60.6 and in 30−44 eV are assigned to those with two holes residing in one of the three Si−F bonds. Strong electrostatic interaction between the two holes confined on the same Si−F bond increases the Auger final state energy and decreases the Auger electron kinetic energy. The Auger final states in 30−44 eV are further split into the triplet and singlet states at 42.0 and 33.0 eV, respectively. Strong localization of the two holes in the same small region of space produces the singlet−triplet splitting in 30−44 eV. As in SiF_4,[29] two-additional moderate peak groups would also appear below an Auger electron kinetic energy of 30 eV (lower limit in our measurement) in FSMSE. Those peak groups could be assigned to Auger final states with two inner valence holes located on different Si−F bonds and to those with two inner holes confined on the same Si−F bond.

4.2.3. Si[Cl]:L_{23}VV AES of CSMSE. Because the Si[Cl]:L_{23}VV AES of CSMSE (Figure 4c) is similar to the Si:L_{23}VV AES of $SiCl_4$ (Figure 4e),[22,32] we have assigned the Si[Cl]:L_{23}VV Auger peaks of CSMSE according to the result of our ab initio MO calculation for $SiCl_4$ (Supporting Information). Note that the hole-localization phenomena seen in SiF_4 were also reported in $SiCl_4$.[32] The assignment for CSMSE is schematically summarized in Figure 6b. The Si[Cl]:L_{23}VV peaks at 75.8 and 67.8 eV (Figure 4c) are assigned to Auger final states with two outer valence holes located on different Si−Cl bonds and to those with two outer holes confined on the same Si−Cl bond, respectively. The Si[Cl]:L_{23}VV Auger peak at 75.8 eV in CSMSE would contain an unresolved component coming from hole creation in higher-lying Si[Cl]−CH_2(bridge) bonding orbitals, just as the Si[F]:L_{23}VV Auger peak at 73.4 eV in FSMSE (Figure 3c) comes from hole creation in higher-lying Si[F]−CH_2(bridge) bonding orbitals.[25] The Si[Cl]:L_{23}VV Auger hump at 59.4 eV in CSMSE (Figure 4c) is assigned to Auger final states with one outer valence hole and one inner hole located on different Si−Cl bonds, though the computational Si[Cl]:L_{23}VV Auger peak around 60 eV in CSMSE is stronger than the experimental one. Any Si[Cl]:L_{23}VV Auger decay producing an Auger electron with a kinetic energy of <55 eV is negligible in CSMSE.

4.3. Transient Period during Which Site Specificity Is Reduced. As mentioned in the Introduction, the F → Cl substitution in $X_3SiC_nH_mSi(CH_3)_3$ (X = F or Cl) reduces the site specificity in the fragmentation caused by the Si[X]:2p

DOI: 10.1021/acs.jpca.6b09399
J. Phys. Chem. A 2016, 120, 9907−9915

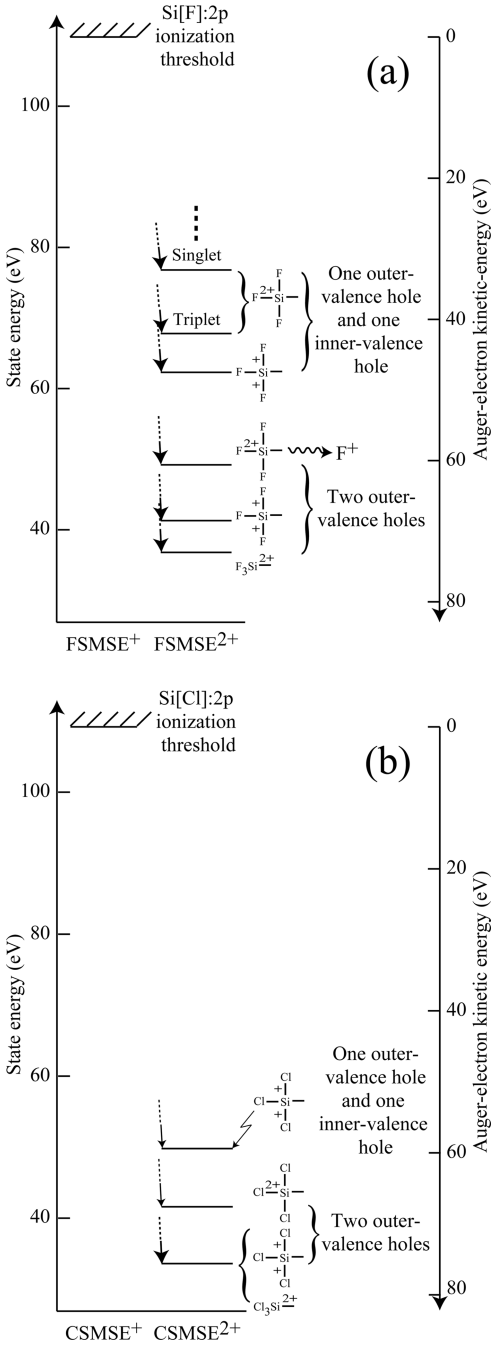

Figure 6. Energy level diagram of singly and doubly charged states related to normal Si[X]:$L_{23}VV$ Auger decays. The straight arrows show major decays. The present AES measurements have been made in an Auger electron kinetic-energy region of >30 eV. (a) FSMSE vapor. As explained in section 4.2.2, some Auger final states would be located also below an Auger electron kinetic energy of 30 eV (see the bold broken line). A previous AEPICO measurement, which was made only above an Auger electron kinetic energy of 54 eV, showed that F^+ ions were produced in the Auger final states at 60.6 eV (see the wavy arrow).[3,6] (b) CSMSE vapor.

ionization. In the present work, by means of the photoelectron Auger electron coincidence spectroscopy, we have attempted to elucidate the transient period during which the site-specificity reduction occurs. Only from the AEPIPICO and AEPICO measurements besides the PEPIPICO and PEPICO ones[3,6] would it be difficult to elucidate it, because the total AES shown in Figures 3a and 4a are not clearly resolved site by site in contrast to the PES shown in Figures 2a and 2b.

As shown in Figures 3 and 4, the Si[X]: and Si[Me]:$L_{23}VV$ AES are very different from each other in each of FSMSE and CSMSE, and so some site specificity in electron relaxation would be maintained during the transient period between the photoelectron and Auger electron emissions. Thus, the site-specificity reduction at the Si[Cl] site of CSMSE is considered to take place during the transient period between the Si[Cl]:$L_{23}VV$ Auger electron emission and the subsequent fragmentation. If a part or the whole of the site-specific fragmentation came from ultrafast dissociation,[20,33] some specificity reduction by the F → Cl substitution should occur during the transient period between the photoelectron and Auger electron emissions. Accordingly, the ultrafast dissociation is unlikely to play a great role in the site-specific fragmentation. This conclusion is consistent with the computational result that little molecular deformation is induced by the Si:2p core−hole formation in FSMSE.[6]

In Figures 3 and 4, the Si[Me]:$L_{23}VV$ AES of FSMSE and CSMSE are close to each other, and similar to that of $Si(CH_3)_4$ vapor.[21,24] However, the Si[X]:$L_{23}VV$ AES of FSMSE and CSMSE are totally different from each other. Furthermore, those are similar to the Si:$L_{23}VV$ AES of SiF_4 and $SiCl_4$ vapors,[20,22,26,32] as mentioned in sections 4.2.2 and 4.2.3. These observations of the Si[XR]:$L_{23}VV$ AES of FSMSE and CSMSE (XR = F, Cl, or Me) would also show that the site specificity is maintained up to the Auger electron emission even in CSMSE.

4.4. Reason for Site-Specificity Reduction. In a previous paper,[3] we noted, "further investigations are needed to clarify the reason for the greater decrease in the Si[X] site specificity (due to the F → Cl substitution in $X_3SiC_nH_mSi(CH_3)_3$ (X = F or Cl))." In the present paper, we have elucidated the reason by adopting the photoelectron Auger electron coincidence technique and by linking the data to the previously obtained results[3,6] in the following way.

F^+ production is the most prominent site-specific fragmentation caused by the Si[F]:2p ionization in FSMSE,[3,6,7] and high site specificity appears in the F^+ production (almost 100% in EPAPS document of ref 6). Because the F^+ production is caused by some violent fragmentation at the Si[F] site, it would take place efficiently in higher-lying Auger final states, to which the Si[F]:$L_{23}VV$ Auger decays of FSMSE considerably lead (Figures 3c and 6a). Furthermore, ionic Si−F bond rupture and the subsequent F^+ production are expected to occur more effectively in an Auger final state with two holes confined on the same Si−F bond than in an Auger final state with two holes located on different Si−F bonds. The Si[F]:$L_{23}VV$ Auger decays of FSMSE lead substantially to the Auger final states with two holes confined on the same Si−F bond, and the efficient site-specific F^+ production actually takes place in these Auger final states (Si[F]:$L_{23}VV$ Auger peak at 60.6 eV).[3,6] In addition, as mentioned in section 4.2.2, the Si[F]:$L_{23}VV$ Auger decays of FSMSE would lead moderately to still higher-lying Auger final states (Auger electron kinetic energy of <30 eV) with two inner valence holes often residing in one of the three Si−F bonds. These Auger decays could also contribute to the efficient site-specific F^+ production. For all these reasons, the site-specific F^+ production in FSMSE is relatively abundant.

In contrast to FSMSE, the Si[Cl]:$L_{23}VV$ Auger decays of CSMSE lead mainly to lower-lying Auger final states (Figures 4c and 6b), in which any violent fragmentation producing Cl^+

DOI: 10.1021/acs.jpca.6b09399
J. Phys. Chem. A 2016, 120, 9907−9915

at the Si[Cl] site would be inactive. Furthermore, because the resultant two holes are not effectively confined on the same Si−Cl bond, ionic Si−Cl bond rupture and the subsequent Cl^+ production would not be active. In addition, the Si[X]:L_{23}VV Auger decay is localized at the Si[X] site as explained in the Introduction, and the Si−Cl bond is much longer than Si−F.[34] Accordingly, valence hole creation on the distant Cl atoms (Cl^+ production) after the localized Si[Cl]:L_{23}VV Auger decay in CSMSE would be less efficient than that on the nearby F atoms (F^+ production) after the similarly localized Si[F]:L_{23}VV Auger decay in FSMSE. For all these reasons, site-specific Cl^+ production in CSMSE is less efficient than the above-mentioned site-specific F^+ production in FSMSE.

On the contrary, site specificity in fragmentation caused by the Si[Me]:2p ionization in CSMSE is similar to, or a little lower than, that in FSMSE,[3,6,7] and Si[Me]-site-specific large fragments containing halogen atoms are produced in both FSMSE and CSMSE. After that, some minor disintegration forming a halogen cation from the Si[Me]-site-specific large fragments seems to occur more in CSMSE than in FSMSE, because the Si−Cl bond is much easier to dissociate than Si−F and the resultant Cl atom is much easier to be ionized than F.[35] In the fragmentation after the Si[Me]:2p ionization of CSMSE, there may be some communication between the Si[Me] and Si[Cl] sites at either end of the molecule, because the Si[Me]-site-specific fragmentation may induce the Si[Cl]−Cl dissociation, leading to the Cl^+ production. Note that the minor disintegration forming the halogen cation from the Si[Me]-site-specific large fragments is not likely to contribute to the maximum Si[Me] site specificity as suggested previously.[3]

Like this, the site-specific Cl^+ production caused by the Si[Cl]:2p ionization in CSMSE is less active than the site-specific F^+ production in FSMSE, whereas the Cl^+ formation through the minor disintegration after the Si[Me]:2p ionization in CSMSE is more active than the corresponding F^+ formation in FSMSE. As a result, the site specificity for the Cl^+ production caused by the Si[Cl]:2p ionization of CSMSE (only ∼50% in Figure S4 of ref 3) is much lower than that for the F^+ production by the Si[F]:2p ionization of FSMSE (almost 100% in EPAPS document of ref 6).

In FSMSE, high site specificity by the Si[F]:2p ionization is also seen in production of SiF^+ and SiF_2^+ ions and SiF^+-containing ion pairs (EPAPS document of ref 6). In contrast, site specificity for production of $SiCl^+$, $SiCl_2^+$, and $SiCl^+$-containing ion pairs is low in the Si[Cl]:2p ionization of CSMSE (Figures S4 and S5 of ref 3). Some minor disintegration forming $SiCl^+$, $SiCl_2^+$, and $SiCl^+$-containing ion pairs from the Si[Me]-site-specific large fragments would again reduce the whole Si[Cl] site specificity of CSMSE.

As mentioned above, the localized Si[Cl]:L_{23}VV Auger decay in CSMSE would not efficiently cause the valence-hole creation on the distant Cl atoms. Instead, the corresponding hole would be created on the Si[Cl] atom itself or the nearby C atom bonded to Si[Cl].[34] The hole creation on the Si[Cl] atom may induce Si[Cl]−CH_2(bridge) dissociation more effectively than it does Si−Cl dissociation, because the Si−C bond energy is less than the Si−Cl one.[35,36] The Si[Cl]−CH_2(bridge) dissociation after the Si[Cl]:L_{23}VV Auger decay would produce some ionic daughter fragments coming from the intersite bridge (−CH_2CH_2−), something containing mono- to trivalent Si[Me], or methyl groups around Si[Me], which are much easier to be ionized than Cl.[35,37] The hole creation on the C atom bonded to Si[Cl] would also form similar daughter fragments. Like this, these daughter fragments are produced through dissociation around the Si[Me] site after the Si[Cl]:L_{23}VV Auger decay, and then the Si[Me] site may, as it were, know what the Si[Cl] site is doing. The daughter fragments would be the same as some minor products formed after the Si[Me]:L_{23}VV Auger decay and the subsequent fragmentation. As a result, we could not distinguish the Si[Cl]-site-specific fragments from the Si[Me]-site-specific ones, and the whole Si[Cl] site specificity would be reduced again in CSMSE.

5. SUMMARY

In our previous site-specific studies performed for $X_3SiC_nH_mSi(CH_3)_3$ by means of the photoelectron, Auger electron, and their ion-coincidence spectroscopies,[3,6,25] the experiments and theory alike relied on some models and assumptions to extract a mechanism (e.g., wavy arrow in Figure 6a) from the raw experimental data. Hence, in spite of the previous successes of those spectroscopies, there was a need for studying the photoelectron Auger electron coincidence spectroscopy capable of yielding observables that are more likely linked to correlation between the photoelectron and Auger electron emissions.[14] Accordingly, we have studied the site-specific electron relaxations caused by the Si:2p core-level photoionizations in FSMSE and CSMSE vapors by means of the photoelectron Auger electron coincidence spectroscopy, and linked the data to the results obtained in our previous works.[3,6,25]

Now we have the answers to the questions asked in the Introduction. When does the site-specificity reduction take place during the relaxation after the Si[Cl]:2p ionization in $Cl_3SiC_nH_mSi(CH_3)_3$? The site-specificity reduction at the Si[Cl] site of $Cl_3SiC_nH_mSi(CH_3)_3$ is considered to take place during the transient period between the Si[Cl]:L_{23}VV Auger electron emission and the subsequent fragmentation. Why does the site specificity in the fragmentation caused by the Si[X]:2p ionization drop much more than that by the Si[Me]:2p ionization in the case that Cl is substituted for F in $X_3SiC_nH_mSi(CH_3)_3$? The reason can be explained in terms of some differences in the experimental results of the Si[X]:L_{23}VV Auger decay between FSMSE and CSMSE. The Si[F]:L_{23}VV Auger decays of FSMSE lead considerably to the higher-lying Auger final states with one or two inner valence holes and to those with two holes confined on the same Si−F bond; in contrast, the Si[Cl]:L_{23}VV Auger decays of CSMSE lead mainly to the lower-lying Auger final states with outer valence holes, which are located mostly on different Si−Cl bonds.

The present work would have brought the goal of controlling chemical reactions at an atomic level and other applications one step closer to realization. The site-specific fragmentation is on the trail of the Holy Grail.

■ ASSOCIATED CONTENT

Supporting Information

The Supporting Information is available free of charge on the ACS Publications website at DOI: 10.1021/acs.jpca.6b09399.

Complete refs 3, 6, 12, and 16; correct Cl:2p photoelectron L_{23}VV Auger electron coincidence spectrum of CSMSE (Figure S1) (PDF)

Assignments of AES peaks based on our ab initio MO calculations for SiF_4 (XLSX)

Assignments of AES peaks based on our ab initio MO calculations for $SiCl_4$ (XLSX)

DOI: 10.1021/acs.jpca.6b09399
J. Phys. Chem. A 2016, 120, 9907−9915

AUTHOR INFORMATION

Corresponding Author

*S. Nagaoka. Phone: 81-89-927-9592. Fax: 81-89-927-9590. E-mail: nagaoka@ehime-u.ac.jp.

ORCID

Shin-ichi Nagaoka: 0000-0003-1564-7328

Notes

The authors declare no competing financial interest.

ACKNOWLEDGMENTS

We express our sincere thanks to Professor Kazuhiko Mase of Institute of Materials Structure Science and to Ms. Megumi Hino of Ehime University for their preliminary measurements of Auger photoelectron coincidence spectra of condensed CSMSE in the early stage of this work. We are grateful to the UVSOR staff for the stable operation of the storage ring and to Dr. Isao H. Suzuki of Institute of Materials Structure Science for his valuable discussion on AES of SiF_4 and $SiCl_4$. We thank the Information Media Center at Hiroshima University for the use of a grid with high-performance PCs, Research Center for Computational Science, Okazaki, Japan, for the use of Fujitsu PRIMERGY, and the Research Institute for Information Technology, Fukuoka, Japan, for the use of Hitachi HA8000tc/HT210. This work was partly supported by JSPS KAKENHI Grant Number 15K04755 and by Shimadzu Science Foundation and Daiko Foundation.

REFERENCES

(1) Hitchcock, A. P.; Neville, J. J. Photoionization Dynamics from Inner-Shell Mass-Spectrometry. In *Chemical Applications of Synchrotron Radiation, Part I: Dynamics and VUV Spectroscopy*; Sham, T.-K., Ed.; World Scientific: Singapore, 2002.

(2) Tanaka, K.; Kizaki, H.; Sumii, R.; Matsumoto, Y.; Wada, S. Atomic Position Dependence of the Primary Core Electron Excitation on Site-Specific Chemical Bond Scission. *Radiat. Phys. Chem.* **2006**, *75*, 2076−2079.

(3) Nagaoka, S.; Fukuzawa, H.; Prümper, G.; Takemoto, M.; Takahashi, O.; Yamaguchi, K.; Kakiuchi, T.; Tabayashi, K.; Suzuki, I. H.; Harries, J. R.; et al. A Study to Control Chemical Reactions Using Si:2p Core Ionization: Site-Specific Fragmentation. *J. Phys. Chem. A* **2011**, *115*, 8822−8831.

(4) Carlson, T. A. *Photoelectron and Auger Spectroscopy*; Plenum: New York, 1975; Section 5.2.

(5) International Technology Roadmap for Semiconductors Home Page. http://www.itrs2.net/ (accessed December 10, 2016).

(6) Nagaoka, S.; Prümper, G.; Fukuzawa, H.; Hino, M.; Takemoto, M.; Tamenori, Y.; Harries, J.; Suzuki, I. H.; Takahashi, O.; Okada, K.; et al. Electron-Ion-Ion Triple-Coincidence Spectroscopic Study of Site-Specific Fragmentation Caused by Si:2*p* Core-Level Photoionization of $F_3SiCH_2CH_2Si(CH_3)_3$ Vapor. *Phys. Rev. A: At., Mol., Opt. Phys.* **2007**, *75*, 020502.

(7) Nagaoka, S.; Takemoto, M.; Prümper, G.; Fukuzawa, H.; Tamenori, Y.; Suzuki, I. H.; Ueda, K. Site-Specific Fragmentation Caused by Core-Level Photoionization in $F_3SiCH_2CH_2Si(CH_3)_3$ Vapor: Comparison between Si:1*s* and 2*p* Photoionizations by Means of Photoelectron-Photoion-Photoion Triple-Coincidence Spectroscopy. *J. Chem. Phys.* **2008**, *129*, 204309.

(8) Nagaoka, S.; Fujibuchi, T.; Ohshita, J.; Ishikawa, M.; Koyano, I. Fragmentation of $F_3SiCH_2CH_2Si(CH_3)_3$ Vapour Following Si:2p Core-Level Photoexcitation. A Search for a Site-Specific Process in Complex Molecules. *Int. J. Mass Spectrom. Ion Processes* **1997**, *171*, 95−103.

(9) http://www.uvsor.ims.ac.jp/beamlines/4B/bl4b.html (accessed December 10, 2016).

(10) Hikosaka, Y.; Sawa, M.; Soejima, K.; Shigemasa, E. A High-Resolution Magnetic Bottle Electron Spectrometer and its Application to a Photoelectron-Auger Electron Coincidence Measurement of the $L_{2,3}VV$ Auger Decay in CS_2. *J. Electron Spectrosc. Relat. Phenom.* **2014**, *192*, 69−74.

(11) Schmidt, V. *Electron Spectrometry of Atoms using Synchrotron Radiation*; Cambridge University Press: Cambridge, 1997; Chapters 4, 6, and 10.

(12) Siegbahn, K.; Nordling, C.; Johansson, G.; Hedman, J.; Hedén, P. F.; Hamrin, K.; Gelius, U.; Bergmark, T.; Werme, L. O.; Manne, R.; et al. *ESCA Applied to Free Molecules*; North-Holland: Amsterdam, 1969; Appendix B.

(13) Thurgate, S. M. Auger Photoelectron Coincidence Experiments from Solids. *J. Electron Spectrosc. Relat. Phenom.* **1996**, *81*, 1−31.

(14) Stefani, G.; Iacobucci, S.; Ruocco, A.; Gotter, R. Electron-Electron Coincidence Spectroscopies at Surfaces. *J. Electron Spectrosc. Relat. Phenom.* **2002**, *127*, 1−10.

(15) Eland, J. H. D.; Vieuxmaire, O.; Kinugawa, T.; Lablanquie, P.; Hall, R. I.; Penent, F. Complete Two-Electron Spectra in Double Photoionization: the Rare Gases Ar, Kr, and Xe. *Phys. Rev. Lett.* **2003**, *90*, 053003.

(16) Frisch, M. J.; Trucks, G. W.; Schlegel, H. B.; Scuseria, G. E.; Robb, M. A.; Cheeseman, J. R.; Scalmani, G.; Barone, V.; Mennucci, B.; Petersson, G. A.; et al. *Gaussian 09*; Gaussian, Inc.: Wallingford, CT, 2010.

(17) Mitani, M.; Takahashi, O.; Saito, K.; Iwata, S. Theoretical Molecular Auger Spectra with Electron Population Analysis. *J. Electron Spectrosc. Relat. Phenom.* **2003**, *128*, 103−117.

(18) Suzuki, I. H.; Nitta, A.; Shimizu, A.; Tamenori, Y.; Fukuzawa, H.; Ueda, K.; Nagaoka, S. Photoelectron Spectra of $F_3SiC_2H_4Si(CH_3)_3$ Molecule Using Monochromatized Synchrotron Radiation. *J. Electron Spectrosc. Relat. Phenom.* **2009**, *173*, 18−23.

(19) Nagaoka, S.; Tanaka, S.; Mase, K. Site-Specific Fragmentation following C:1s Core-Level Photoionization of 1,1,1-Trifluoroethane Condensed on a Au Surface and of a 2,2,2-Trifluoroethanol Monolayer Chemisorbed on a Si(100) Surface. *J. Phys. Chem. B* **2001**, *105*, 1554−1561.

(20) Suzuki, I. H.; Kono, Y.; Ikeda, A.; Oi, M.; Ouchi, T.; Ueda, K.; Tamenori, Y.; Takahashi, O.; Nagaoka, S. Cascade Auger Decays Following Si $KL_{23}L_{23}$ Auger Transition in SiF_4. *J. Chem. Phys.* **2013**, *138*, 024302.

(21) de Souza, G. G. B.; Platania, R.; de A. e Souza, A. C.; Maracci, F. Chemical State Effect in the Auger (C KVV and Si LVV) Spectra of Hexamethyldisilane. *Chem. Phys.* **1989**, *129*, 491−494.

(22) Suzuki, I. H.; Bandoh, Y.; Mochizuki, T.; Fukuzawa, H.; Tachibana, T.; Yamada, S.; Takanashi, T.; Ueda, K.; Tamenori, Y.; Nagaoka, S. Molecular Cascade Auger Decays Following Si $KL_{23}L_{23}$ Auger Transitions in $SiCl_4$. *J. Phys. B: At., Mol. Opt. Phys.* **2016**, *49*, 165102.

(23) Mase, K.; Kobayashi, E.; Nambu, A.; Kakiuchi, T.; Takahashi, O.; Tabayashi, K.; Ohshita, J.; Hashimoto, S.; Tanaka, M.; Nagaoka, S. Site-Specific Ion Desorption from Condensed $F_3SiCD_2CH_2Si(CH_3)_3$ Induced by Si-2p Core-Level Ionizations Studied with Photoelectron Photoion Coincidence (PEPICO) Spectroscopy, Auger Photoelectron Coincidence Spectroscopy (APECS) and Auger Electron Photoion Coincidence (AEPICO) Spectroscopy. *Surf. Sci.* **2013**, *607*, 174−180.

(24) de Souza, G. G. B.; Morin, P.; Nenner, I. Angle Resolved Photoelectron Study of Resonances near the Si 2*p* Edge of the $Si(CH_3)_4$ Molecule. *J. Chem. Phys.* **1985**, *83*, 492−498.

(25) Nagaoka, S.; Nitta, A.; Tamenori, Y.; Fukuzawa, H.; Ueda, K.; Takahashi, O.; Kakiuchi, T.; Kitajima, Y.; Mase, K.; Suzuki, I. H. Auger Electron Spectra of $F_3SiCH_2CH_2Si(CH_3)_3$ Obtained by Using Monochromatized Synchrotron Radiation. *J. Electron Spectrosc. Relat. Phenom.* **2009**, *175*, 14−20.

(26) Aksela, S.; Tan, K. H.; Aksela, H.; Bancroft, G. M. Si(*LVV*) Auger and Resonance Auger Spectra of SiF_4 Molecules with the Use of Synchrotron Radiation. *Phys. Rev. A: At., Mol., Opt. Phys.* **1986**, *33*, 258−263.

DOI: 10.1021/acs.jpca.6b09399
J. Phys. Chem. A 2016, 120, 9907−9915

(27) Nagaoka, S.; Mase, K.; Nagasono, M.; Tanaka, S.; Urisu, T.; Ohshita, J. Site-Specific Fragmentation Following Si:2p Core-Level Photoionization of $F_3SiCH_2CH_2Si(CH_3)_3$ Condensed on a Au surface. *J. Chem. Phys.* **1997**, *107*, 10751−10755.
(28) Tarantelli, F.; Cederbaum, L. S. Foreign Imaging in Auger Spectroscopy: The Si 2*p* Spectrum of Silicon Tetrafluoride. *Phys. Rev. Lett.* **1993**, *71*, 649−652.
(29) Gottfried, F. O.; Cederbaum, L. S.; Tarantelli, F. *Ab Initio* Block-Lanczos Calculation of the Auger Spectra of SiF_4: Strong Two-Hole Localization Effects and Foreign Imaging. *Phys. Rev. A: At., Mol., Opt. Phys.* **1996**, *53*, 2118−2129.
(30) Tarantelli, F.; Sgamellotti, A.; Cederbaum, L. S. Many Dicationic States and Two-Hole Population Analysis as a Bridge to Auger Spectra: Strong Localization Phenomena in BF_3. *J. Chem. Phys.* **1991**, *94*, 523−532.
(31) For example, see: Slavíček, P.; Kryzhevoi, N. V.; Aziz, E. F.; Winter, B. Relaxation Processes in Aqueous Systems upon X-ray Ionization: Entanglement of Electronic and Nuclear Dynamics. *J. Phys. Chem. Lett.* **2016**, *7*, 234−243.
(32) Aksela, A.; Sairanen, O.-P.; Aksela, H.; Bancroft, G. M.; Tan, K. H. Normal and Resonance *LVV* Auger Spectra of Gas-Phase $SiCl_4$ Molecules. *Phys. Rev. A: At., Mol., Opt. Phys.* **1988**, *37*, 2934−2940.
(33) Morin, P.; Nenner, I. Atomic Autoionization Following Very Fast Dissociation of Core-Excited HBr. *Phys. Rev. Lett.* **1986**, *56*, 1913−1916.
(34) *Landort-Börnstein*; Hellwege, K.-H., Ed.; Springer-Verlag: Berlin, 1976; Vol. 7. A typical Si−Cl bond is longer than Si−F and Si−C by no less than 0.43 and 0.14 Å, respectively.
(35) Pimentel, G. C.; Spratley, R. D. *Chemical Bonding Clarified through Quantum Mechanics*; Holden-Day: San Francisco, 1969; Appendix. The Si−Cl bond energy is only ∼2/3 of the Si−F one, and the ionization energy of Cl is only ∼3/4 of that of F.
(36) Davidson, I. M.; Stephenson, I. L. Bond Dissociation Energies of Trimethylsilyl Compounds. *Chem. Commun.* **1966**, 746−748. A typical Si−C bond energy is ∼83% of the Si−Cl bond energy given in ref 35.
(37) Dyke, J.; Jonathan, N.; Lee, E.; Morris, A. Vacuum Ultraviolet Photoelectron Spectroscopy of Transient Species. Part 7.−The Methyl Radical. *J. Chem. Soc., Faraday Trans. 2* **1976**, *72*, 1385−1396. For example, the ionization energy of CH_3 is only ∼76% of that of Cl given in ref 35.

DOI: 10.1021/acs.jpca.6b09399
J. Phys. Chem. A 2016, 120, 9907−9915